JOURNAL OF AIRCRAFT
Vol. 30, No. 2, March–April 1993

Simultaneous Structure/Control Design Optimization of a Wing Structure with a Gust Load Alleviation System

Shinji Suzuki*
University of Tokyo, Tokyo 113, Japan
and
Satoshi Yonezawa†
Kobe Steel, Ltd., Hyogo 651-22, Japan

Simultaneous design optimization is considered for structure and control parameters of a wing with a gust load alleviation (GLA) control system. The application of a goal programming (GP) formulation to the design synthesis of an aeroservoelastic system is carried out by the use of a simple mathematical model in conjunction with a wind-tunnel model having a GLA control system. Numerical applications are based on a cantilever wing having an aileron surface controlled by wing-tip accelerometer feedback signals. System equations are obtained in the form of state equations, thus enabling the statistical characteristics of both the gust-induced wing stress and the control surface deflection angle to be evaluated using their standard deviations. The wing spar height and the controller feedback gain are simultaneously optimized to obtain the minimum spar weight while satisfying the following structure and control design constraints: 1) the spar stress is limited with the control system either on or off; 2) the control surface deflection angle is restricted; and 3) system stability should be guaranteed by incorporating a controller stability margin. Numerical examples demonstrate the successful application of a GP formulation for the simultaneous structure/control design synthesis by specifying priorities to the conflicting design constraints.

Introduction

ACTIVE control technology has been recognized as a design tool to improve aeroelastic characteristics of flight vehicles.[1] Active controls have been attempted into aircraft to improve structural deficiency, to increase fatigue life, and/or suppress aeroelastic instabilities without increasing structural weight. This design process primarily depends on the control system's design and traditionally no modifications can be applied to the structure. However, due to the strong interactions between these two systems, a simultaneous design synthesis method must be developed at an early stage of vehicle design in order to take full advantage of active control techniques.[2] This led to the present article which describes a simultaneous structure/control design optimization method for a wing having a gust load alleviation (GLA) control system.[3]

Numerical optimization of simultaneous structure/control design synthesis has been successfully applied to structures in space[4]; however, aircraft design applications are limited as a result of complex design requirements, e.g., control systems must have sufficient stability margins, and aircraft structures must withstand load conditions when used with the control system including control system failure. As a result, the minimum structural weight design subject to gust load constraints usually considers structures with no control system,[5–7] and has led to the development of control design synthesis methods for alleviating gust loads which only consider existing structures without modifications.[8,9] Recently, simultaneous structure/control design synthesis for an active flutter suppression system in simplified models was reported,[10,11] and sensitivities of flutter characteristics and stability margins with respect to structure/control design parameters were derived.[12] However, more effort must be directed toward simultaneous structure/control optimization in aircraft design.

Received Sept. 3, 1991; revision received Nov. 19, 1991; accepted for publication Jan. 24, 1992.

*Associate Professor, Department of Aeronautics, 7-3-1 Bunkyo-ku, Hongo. Member AIAA.

†Graduate Student, Research Engineer, Mechanical Engineering Research Laboratories, 1-5-5 Takatsukadai, Nishi-ku, Kobe.

Simultaneous structure/control optimization generally considers multiple objective optimization problems since the structure and control problems have either individual design requirements or constraints, and in practical situations criteria target values of achievement are of significance. Here, goal programming (GP) is applied to optimize the structure/control design parameters for wing structures incorporating a GLA system. GP considers design objectives as achievement goals by using priority classifications to solve conflicting multiple goals.[13] Although GP is an important technique for multiple criteria optimization in mathematical economics, this approach is not commonly used in engineering fields.[11] This approach is sequentially applied to a linearized problem to obtain the optimum structure/control design parameters since the simplex algorithm can efficiently and reliably solve linearized GP problems. The following design requirements are considered: 1) system stability requirements incorporating stability margins; 2) gust-induced stress constraints with the control system on or off; 3) restriction of the control surface deflection angle; and 4) minimization of structure weight.

To demonstrate the sequential GP approach, a simple aeroservoelastic system is utilized. Numerical applications are based on a wind-tunnel model designed to experimentally study the GLA control system.[3] Although gust loads have been previously analyzed in the frequency domain, this study considers the system equations as a first-order time-domain (state-space) form, thereby enabling modern control design techniques to be utilized. The presented method is summarized as follows: 1) vertical gust velocities are represented as output signals of a first-order state equation driven by Gaussian white noise; 2) the standard deviation of the principal bending stress is used to evaluate the gust-induced stress; and 3) a conventional feedback control law is applied to move the aileron control surface using wing-tip accelerometer measurements. It should be noted that it is difficult to use statistical properties which consider more sophisticated fatigue criteria involving combinations of stress components since the phase relations between the stress components cannot be obtained. However, Ref. 7 proposed the use of constraints based on an equal-probability-of-load-combination to cope with this difficulty.

Selected design parameters are the wing spar height distribution and the controller feedback gain which are then optimized to obtain the minimum spar weight while satisfying all structure and control system design requirements.

Aeroservoelastic Model

Aeroelastic Model

A wind-tunnel model used is shown in Fig. 1, being a uniform cantilever wing having an aileron surface for active control which is vertically attached to the wind-tunnel wall at a 0 deg angle of attack.

The wing spar is divided into bar elements for finite element method (FEM) structural analysis. An airfoil covering the spar and an actuator device are modeled as concentrated mass and inertia added to each nodal point. The controller device mass and location are fixed in this study because an available actuator device and its location were limited in this wind-tunnel model. It should be noted that the controller device size should be changed according to the control output, and also that its location should be selected as a design variable since both its mass and placement directly influence structure's dynamic characteristics.

Time domain equations for dynamic response of the wing spar structure are

$$[I]\{\ddot{\xi}\} + [B_s]\{\dot{\xi}\} + [K_s]\{\xi\} = \{f\} \tag{1}$$

where $[I]$, $[B_s]$, and $[K_s]$ are the identity, damping, and stiffness matrices, respectively, $\{\xi\}$ is the generalized structural displacement vector, and $\{f\}$ is the generalized force vector associated with air forces. The physical displacement vector $\{z\}$ is represented as

$$\{z\} = [\Phi]\{\xi\} \tag{2}$$

where $[\Phi]$ is the matrix of eigenvectors normalized with the generalized mass matrix. The present mathematical model consist of three modes, i.e., the first and second bending modes and a spar torsion mode.

A simple aerodynamic model is used in this study. The air forces acting on a wing section are approximated by the quasi-steady two-dimensional potential flow theory including an apparent mass effect, whereas the air forces due to a control surface deflection are estimated using the steady aerodynamic theory. The reason for using this simple aerodynamic model is that the reduced frequency of the original wind-tunnel model is low, therefore allowing the analytical derivation of aerodynamic loads derivatives with respect to design parameters. The bending frequency ω and the reduced frequency k ($=\omega b/U$; b is a semichord, and U is a flow velocity) of the baseline wind-tunnel model were 6.12 rad/s and 0.0459, respectively.

Integration of the section forces using the strip theory will result in the generalized force vector

$$\{f\} = \{H_\alpha\}\alpha_g + \{H_\delta\}\delta + [H_1]\{\ddot{\xi}\} + [H_2]\{\dot{\xi}\} + [H_3]\{\xi\} \tag{3}$$

where $[H_1]$, $[H_2]$, and $[H_3]$ are aerodynamic matrices related to the generalized coordinates, and $\{H_\alpha\}$ and $\{H_\delta\}$ are aerodynamic vectors generated by a wind gust having an angle-of-attack α_g and by the aileron deflection angle δ, respectively.

Gust Model

A random wind gust with a vertical velocity w_g is modeled using output signals of the first-order time domain equation

$$\dot{w}_g = -\omega_g w_g + \omega_g n_g \tag{4}$$

where ω_g and n_g are a cutoff frequency of the gust model and the Gaussian white noise, respectively. The variance of the gust velocity is

$$E[w_g^2] = (\omega_g V_g/2) \tag{5}$$

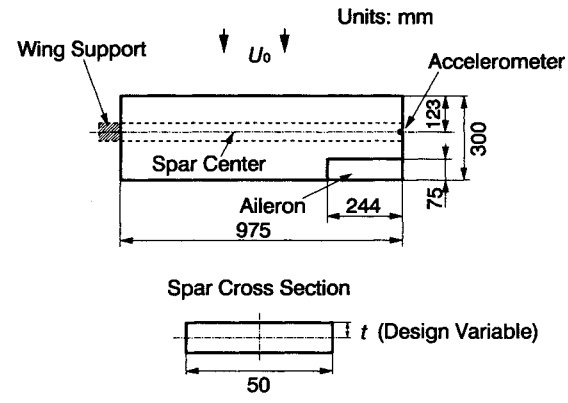

Fig. 1 Cantilever wing with control surface.

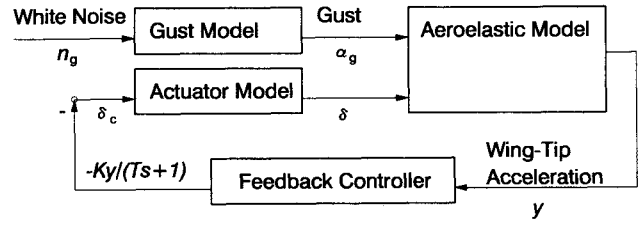

Fig. 2 Feedback control system.

where V_g is the intensity of the white noise. The gust angle-of-attack α_g in Eq. (3) is represented by w_g/U_0.

Control Model

The actuator transfer function is

$$\frac{\delta}{\delta_c} = \frac{\omega_c^2}{s^2 + 2\zeta_c\omega_c s + \omega_c^2} \tag{6}$$

where δ and δ_c are the aileron surface deflection angle and a command signal to the actuator, ζ_c and ω_c are dynamic characteristics of the actuator, and s is the Laplace variable.

The value of δ_c is determined by feedback signals from a wing-tip mounted accelerometer (Fig. 1), with the negative feedback control law being defined as

$$\delta_c = -[-K(Ts + 1)]y \tag{7}$$

where T and K are a time constant and the controller feedback gain, respectively, and y is the wing-tip vertical acceleration. Figure 2 shows a block diagram of the closed loop feedback control system. Since the aeroelastic model's transfer function between δ and y is negative, the sign of the feedback gain is made negative so that the open loop transfer function between the command signal δ_c and the controller's feedback signal $-Ky/(Ts + 1)$ is positive. To increase the damping of the first bending mode, the phase angle between δ and y is adjusted to be 90 deg at the first bending mode frequency ω_1 by setting the time constant T equal to

$$T = \frac{\omega_c^2 - \omega_1^2}{2\zeta_c\omega_c\omega_1^2} \tag{8}$$

The wing-tip vertical acceleration y can be written as

$$y = \{\phi_{\text{tip}}\}^T\{\ddot{\xi}\} \tag{9}$$

where $\{\phi_{\text{tip}}\}$ is the vector containing each eigenvector component at the wing tip.

System Equations

Transforming Eq. (6) into a state-space form by combining Eqs. (1), (3), and (4) results in the open loop equations

$$\begin{aligned} \{\dot{x}\} &= [A]\{x\} + \{B\}\delta_c + \{D\}n_g \\ y &= \{C\}^T\{x\} \end{aligned} \tag{10}$$

where

$$\{X\}^T = \{\xi^T, \dot{\xi}^T, \alpha_g, \delta, \dot{\delta}\} \tag{11}$$

$$[A] = \begin{bmatrix} 0 & I & 0 & 0 & 0 \\ -M_p^{-1}K_p & -M_p^{-1}B_p & M_p^{-1}H_\alpha & M_p^{-1}H_\beta & 0 \\ 0 & 0 & -\omega_g & 0 & 0 \\ 0 & 0 & 0 & 0 & 1 \\ 0 & 0 & 0 & -\omega_c^2 & -2\zeta_c\omega_c \end{bmatrix} \tag{12}$$

with

$$M_p = I - H_1,\ B_p = B_s - H_2,\ K_p = K_s - H_3 \tag{13}$$

$$\{B\}^T = \{0, 0, 0, 0, \omega_c^2\} \tag{14}$$

$$\{D\}^T = \{0, 0, \omega_g/U_0, 0, 0\} \tag{15}$$

$$\{C\}^T = \{0, \phi_{\text{tip}}^T, 0, 0, 0,\}[A] \tag{16}$$

The open loop Eq. (10) can be closed by using the feedback control law [Eq. (7)], which results in the closed loop state equations

$$\{\dot{x}_c\} = [A_c]\{x_c\} + \{D_c\}n_g \tag{17}$$

where

$$\{x_c\} = \begin{Bmatrix} x \\ \delta_c \end{Bmatrix} \tag{18}$$

$$[A_c] = \begin{bmatrix} A & B \\ (K/T)C^T & -1/T \end{bmatrix} \tag{19}$$

$$\{D_c\} = \begin{Bmatrix} D \\ 0 \end{Bmatrix} \tag{20}$$

having a total order of 10.

If the system is stable, the steady-state covariance matrix is defined as

$$[Q] = \lim_{t\to\infty} E[x_c x_c^T] \tag{21}$$

where $[Q]$ is solved by the Lyapunov matrix equation[14]

$$[A_c][Q] + [Q][A_c]^T + \{D_c\}V_g\{D_c\}^T = 0 \tag{22}$$

with V_g being the intensity of the input white nose n_g in Eq. (5).

The FEM formulation can evaluate the stress of each element as[15]

$$\{\sigma\} = [S]\{z\} \tag{23}$$

where $\{\sigma\}$ and $[S]$ are the stress vector at each element and the transformation matrix, respectively. The covariance matrix associated with the stress vector is defined as

$$[Q_\sigma] = [S][\Phi][Q_\xi][\Phi]^T[S]^T \tag{24}$$

where $[Q_\xi]$ is the covariance matrix for the state ξ.

Stability Index

In order to assure system stability, a stability index is introduced as[10]

$$F_s = \frac{1}{\rho_s} \ln\left(\sum_{i=1}^{N} e^{\rho_s\lambda_i}\right) \tag{25}$$

where N is the order of the system; λ_i is the real part of the ith eigenvalue of the system matrix $[A_c]$, and ρ_s is a scaling parameter. Equation (25) is the Kreisselmeier-Steinhauser function,[16] and when $F_s < 0$, the system is stable.[10]

Although a condition of $F_s < 0$ guarantees system stability, the control system still may not have sufficient stability margins. Therefore, in the following applications, the system is considered stable even if the feedback gain increases the design variable by up to 3.16 times, being represented as

$$F_s(3.16K) < 0 \tag{26}$$

with Eq. (26) indicating that the control system has a gain margin of greater than 10 dB.

Goal Programming

Design parameters of the aeroservoelastic system were selected as structural parameters for each element in the FEM formulation and the feedback gain K in Eq. (7). These parameters p_i ($i = 1, \ldots, N_d$) are optimized to minimize the wing structural weight $M(p_i)$ while also satisfying the corresponding design constraints.

The design problem can be expressed as a general nonlinear optimization problem

$$\begin{aligned} &\text{minimize:} && M(p_i) \\ &\text{subject to:} && c_j(p_i)\{\leq, =, \geq\}b_j \\ &&& (\text{for } i = 1, \ldots, N_d) \\ &&& (\text{for } j = 1, \ldots, N_c) \end{aligned} \tag{27}$$

where $c_j(p_i)$ are N_c constraint functions. In the structure design the constraint functions represent restrictions on both the maximum stress and the design variables' upper/lower limits, whereas the control design considers the stability requirements and restrictions on the control surface deflection angle.

Since many design constraints appearing in Eqs. (27) are not satisfied in the original baseline wind-tunnel model, and since no feasible solutions satisfying all design constraints may be found, it should be considered that each criterion has a target value of achievement. Additionally, each criterion has a priority of significance in an engineering sense. The GP approach[13] is considered to be suitable for this optimization problem because it minimizes as best as possible the deviations from target values in accordance with the priority, thereby obtaining solutions even if all constraints are not satisfied. GP deals with a constraint value b_j in Eq. (27) as a goal value g_j and defines deviation variables d_j^+ and d_j^- to measure overachievement and underachievement from the target goal g_j. Considering the original objective function M has an ideal goal g_{N_c+1} the following relations are obtained:

$$\begin{aligned} &\text{subject to:} && f_k(p_i) - d_k^+ + d_k^- = g_k \\ &&& d_k^+ \cdot d_k^- = 0 \\ &&& d_k^+ \geq 0,\ d_k^- \geq 0 \\ &&& (\text{for } i = 1, \ldots, N_d) \\ &&& (\text{for } k = 1, \ldots, N_c + 1) \end{aligned} \tag{28}$$

In a GP formulation, an objective function to be minimized is given as

$$\text{minimize:} \quad \sum_{l=1}^{L}\left[P_l\left(\sum_{k\in l}(w_k^+ d_k^+ + w_k^- d_k^-)\right)\right] \tag{29}$$

where P_l represents the priority of the goals, and w_k^+ and w_k^- are weights in the same priority level I_l. The goals are grouped according to priorities. The goals at the upper priority level are considered to be infinitely more important than goals at the lower priority level; thus, P_l does not represent a real number but indicates the goal at priority level l. This means that the objective functions at the lower priority level can only be further minimized by not decreasing the objective functions

at the upper priority. An appropriate choice of w_k^+ and w_k^- makes it possible to deal with various types of design requirements, e.g., inequality constraints, equality constraints, and function minimization (see Table 1).

If the goal function f_k is a linear function with respect to a parameter p_i, the GP formulated problem can efficiently be solved by the modified simplex algorithm (the lexicographical simplex algorithm[13]). Therefore, f_k is linearized with respect to the design variables so that the algorithm can obtain the optimal solutions within the move limits of each design variable. The objective function in Eqs. (28) is then linearized for each successive updated design variable until all solutions converge. A proper choice of the move limits is required to assure the linearity assumption of f_k and to converge the iteration process. Typically, a proper choice for the starting value of the move limits is 10% of an initial design parameter. These values are reduced when a design parameter changes its sign during the iteration process. Note that this situation can also be found in a conventional sequential linear programming approach.[17]

Sensitivity Analysis

A derivative of the goal function with respect to the design parameter must be calculated in each design cycle. It was found that a sensitivity analysis which analytically determines the derivatives improves the computational efficiency.

The derivatives with respect to a design parameter p for the covariance matrix $[Q]$ and the stress matrix $[S]$ are used to obtain stress and the control surface deflection angle derivatives. The derivative matrix $\partial[Q]/\partial p$ can be calculated from the Lyapunov equation

$$[A_c]\frac{\partial[Q]}{\partial p} + \frac{\partial[Q]}{\partial p}[A_c]^T + \frac{\partial[A_c]}{\partial p}[Q] + [Q]\frac{\partial[A_c]^T}{\partial p} = 0 \tag{30}$$

obtained from Eq. (22). The calculation of the derivative matrix $\partial[A_c]/\partial p$ in Eq. (30) requires derivatives of the structure matrices $[B_s]$ and $[K_s]$ in Eqs. (1), the aerodynamic matrices and vectors in Eq. (3), the time constant T in Eq. (8), and the output matrix $[C]$ in Eq. (10). These derivatives are calculated using both the structure's eigenfrequency derivative and the structure's eigenvector derivative obtained in the FEM structural analysis.[18]

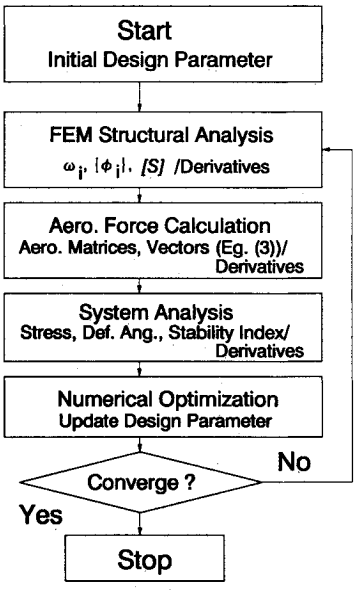

Fig. 3 Optimization procedure flowchart.

Table 1 Weight selections in goal programming

Weight	Constraint or objective
$w_k^+ > 0, w_k^- > 0$	Subject to: $f_k(p_i) = g_k$
$w_k^+ > 0, w_k^- = 0$	Subject to: $f_k(p_i) \leq g_k$
$w_k^+ = 0, w_k^- > 0$	Subject to: $f_k(p_i) \geq g_k$
$w_k^+ > 0, w_k^- < 0$	Minimize: $f_k(p_i)$

It is necessary to determine the derivative with respect to a design parameter for the eigenvalue of the system matrix $[A_c]$ in order to calculate the derivatives of the stability index F_s. The derivative of the eigenvalue λ_i is[19]

$$\frac{\partial\lambda_i}{\partial p} = \{l_i\}^T\frac{\partial[A_c]}{\partial p}\{r_i\} \tag{31}$$

where $\{l_i\}$ and $\{r_i\}$ are the ith left and right eigenvectors of the system matrix $[A_c]$.

As shown in Fig. 3, the presented design procedure is summarized as follows: 1) define initial design parameters; 2) calculate structural characteristics, i.e., the eigenfrequency ω_i, the eigenvector $\{\phi_i\}$, the stress matrix $[S]$ in Eq. (23), and their derivatives; 3) compute the aerodynamic matrices and vectors, i.e., $[H_1]$, $[H_2]$, $[H_3]$, $[H_\alpha]$, and $\{H_\delta\}$, in Eq. (3) and their derivatives; 4) assemble the system equations and calculate the system characteristics with the control system on and off, i.e., the standard deviations of both the element stress and the control surface deflection angle, the stability index, and their derivatives; 5) make the linear model for the GP formulation and obtain the optimized design parameters within their move limits; and 6) update the design parameters and return to step 2) until all solutions converge.

Numerical Example

Mathematical Model

The design objective in numerical applications is to find the optimum spar height t of each bar element and the optimum feedback gain K in Eq. (7) which minimize the spar weight while satisfying structure and control design requirements. Table 2 summarizes the material properties and numerical parameters used in the problem. Note that the spar is divided into eight bar elements and the number of design parameters is nine.

Structural Optimization

A conventional design procedure is initially applied (i.e., only the structural design parameters are optimized without considering the control system), and then controller feedback gain is adjusted to reduce gust-induced stress of the obtained structure.

The maximum stress from a wind gust must be limited to prevent unacceptable structure fatigue, and should be defined under the conditions with the control system on and off in case of a control system failure. Although structure fatigue criteria define these maximum stresses in aircraft structures, the present study introduced control system on/off limits using the stress levels determined by the wind-tunnel model (Fig. 1), e.g., the maximum principal stress with the control system

Table 2 Material properties and numerical parameters

Parameter		Value
Spar material property	Young's modulus	71.5, GPa
	Poisson's ratio	0.335
	Density	2.79×10^3, kg/m^3
Uniform flow	Velocity (U_0)	20, m/s
	Density	1.225, kg/m^3
Gust model [Eq. (4)]	ω_g	0.333, Hz
	Variance ($E[w_g^2]$)	0.0324, (m/s)^2
Actuator model [Eq. (6)]	ω_c	6.0, Hz
	ζ_c	0.7
Scaling parameter [Eq. (25)]	ρ_s	10

on is 3.0 MPa and the maximum one with the system off is relaxed up to 4.5 MPa.

Based on the maximum allowable stress constraint, the structure with the control system off is optimized under the prioritized design goals shown in Table 3. The first priority concerns the upper and lower limits of the spar height, the second priority considers the maximum stress requirement with the control system off, and the third one (the reduction of the spar weight) is satisfied as best as possible without decreasing the other two priorities. The initial spar height of each element was set to 3.0 mm.

Figure 4 shows the design cycle histories of the objective functions, where the stress of the root element is divided by the goal value (4.5 MPa) and the weight is divided by the optimized minimum weight (0.489 kg). The stress requirement (the second priority) is satisfied early, then the spar weight (the third priority) is reduced without violating the maximum stress. Figure 5 shows the iteration histories of the element spar height and the standard deviation of the principal stress. The spar height is larger at the root section and smaller at the tip section to obtain the maximum stress level along the wing span.

The control system can further reduce the spar stress obtained in the structural optimization. The controller's stress reduction performance is shown in Fig. 6 with respect to the feedback gain (the controller design parameter) vs the stan-

Table 3 Optimization goals (structure optimization with control system off)

Priority	Objective
1	$1.0 \le t \le 6.0$, mm
2	$D[\sigma]^a \le 3.0$, MPa
3	Minimize weight

[a] $D[\sigma]$ Denotes the standard deviation of a parameter.

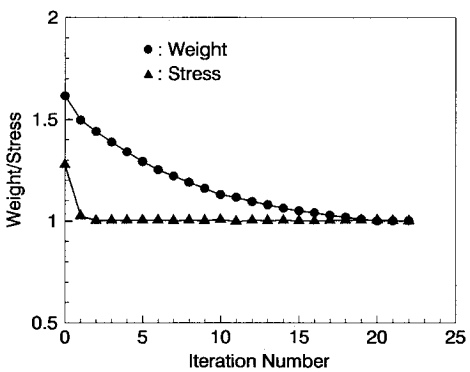

Fig. 4 Normalized weight and stress (root element) vs iteration number (structure optimization).

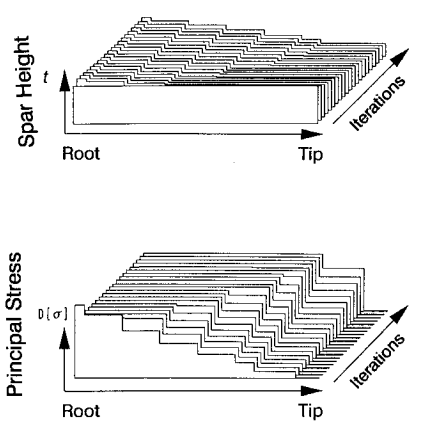

Fig. 5 Design cycle history of spar height and principal stress (structure optimization with the control system off).

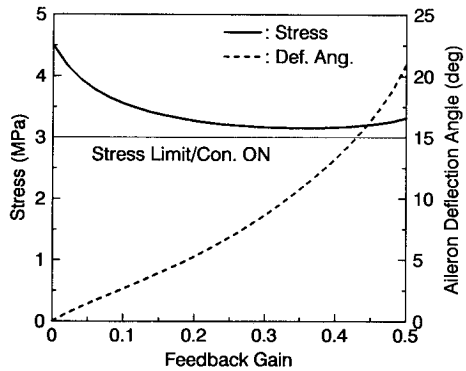

Fig. 6 Maximum stress and aileron deflection angle vs feedback gain.

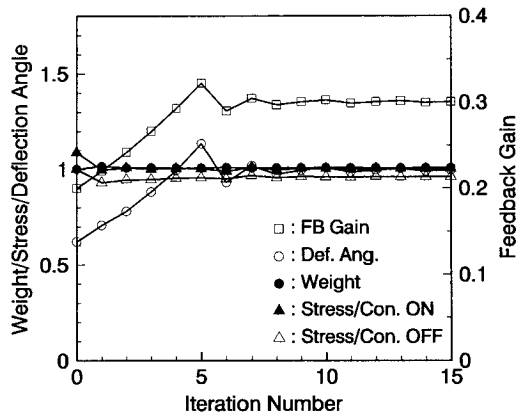

Fig. 7 Normalized weight, stress of root element (control system on/off), aileron deflection angle, and feedback gain vs iteration number (structure/control optimization without stability margin).

Table 4 Optimization goals (structure/control optimization with control system on/off)

Priority	Objective
1	$1.0 \le t \le 6.0$, mm
2	$F_s < 0.0$
3	$D[\sigma_c]^a \le 3.0$, MPa
4	$D[\delta]^a \le 8.5$, deg
5	$D[\sigma_{nc}]^a \le 4.5$, MPa
6	Minimize weight

[a] $D[\sigma_c, \delta, \sigma_{nc}]$ Denotes the standard deviation of a parameter.

dard deviations of the maximum stress and the aileron deflection angle. The design procedure cannot reduce the maximum stress below the allowable limit (3.0 MPa) because the system becomes unstable by increasing the feedback gain; thus, the control system's effectiveness is diminished at higher control gains.

Structure/Control Optimization

In the next step, both the structure design parameters and the feedback gain are simultaneously optimized.

Table 4 shows the prioritized design goals, where the second priority is the system stability requirement, the third priority is the allowable stress limit with control system on, the fourth priority indicates the aileron's maximum deflection angle, the fifth priority is defined for the allowable stress limit with control system off, and the final priority is for the weight reduction. The initial spar height (the structure design parameter) was set at the optimized value from Fig. 5, whereas the initial feedback gain (the control design parameter) was set to 0.2.

Figure 7 shows the design cycle histories in which the weight is normalized by an initial value (0.489 kg), the stresses with the control system on and off are divided by their allowable

limits (3.0 MPa and 4.5 MPa) respectively, and the aileron deflection angle is divided by its maximum limit (8.5 deg). The stress requirement can be satisfied early, with the feedback gain subsequently increasing to minimize the spar weight as best as possible until the aileron deflection angle reaches its allowable limit. However, the weight reduction due to the increase of the feedback gain is slight, and the high controller gain is unsuitable with respect to system stability characteristics.

Figure 8 shows the optimized system's Nyquist plot of the open-loop transfer function between the actuator command signal δ_c and the feedback control signal $-Ky/(Ts + 1)$. The distance between the point $(-1, 0)$ and the system's open-loop transfer function indicates a controller stability margin. Although the system is stable, it does not have a sufficient stability margin, thus an additional constraint for the stability margin must be incorporated.

Structure/Control Optimization with Stability Margin

To assure an adequate stability margin, the following design constraint was introduced: maintaining the system margin by allowing the feedback gain to increase the design variable by up to 3.16 times, i.e., having a control system gain margin of greater than 10 dB. This stability margin constraint [Eq. (26)] was included in the design procedure as the second priority of Table 4.

The design cycle histories of the objective functions are illustrated in Fig. 9, and even though the weight converges to a larger value (0.502 kg) than the initial one (0.489 kg), the feedback gain and the aileron deflection angle are maintained small. This optimized system has sufficient stability margin because the gain and phase margins are over 10 dB and 80 deg as shown in the Nyquist plot of the open-loop transfer function (Fig. 10).

Finally, to check the uniqueness of the solutions, the design process with the same design requirements was executed from different starting points, i.e., the initial spar was selected as a uniform spar having 3.0-mm height. Figure 11 shows the design cycle histories in which each item is normalized by the same value used in Fig. 9. It should be noted the solutions converge to the same values obtained in Fig. 9. Figure 12

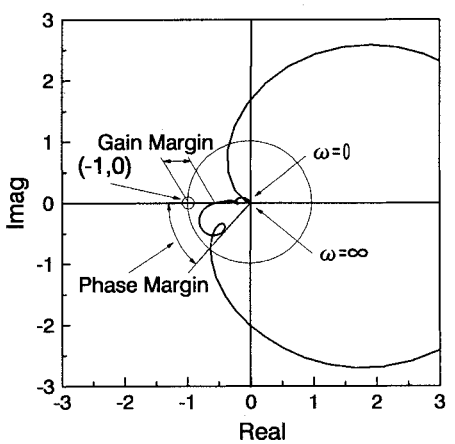

Fig. 8 Nyquist plot of open-loop transfer function (optimum design without stability margin).

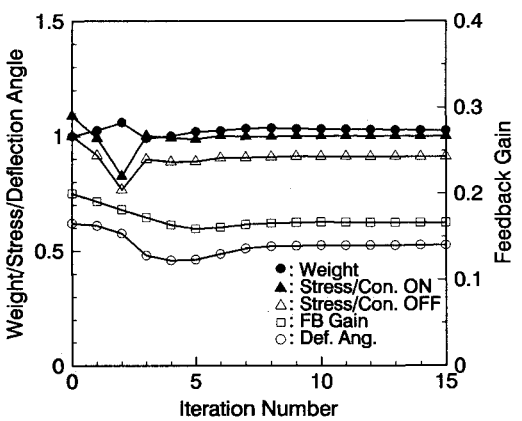

Fig. 9 Normalized weight, stress of root element (control system on/off), aileron deflection angle, and feedback gain vs iteration number (structure/control optimization with stability margin).

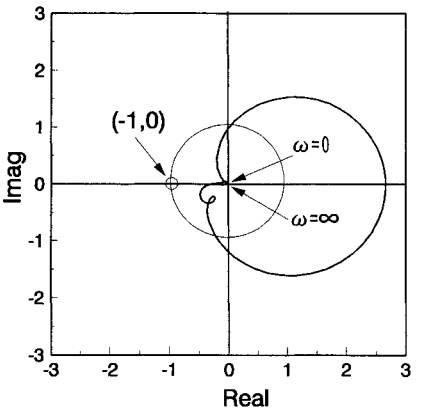

Fig. 10 Nyquist plot of open-loop transfer function (structure/control optimization with stability margin).

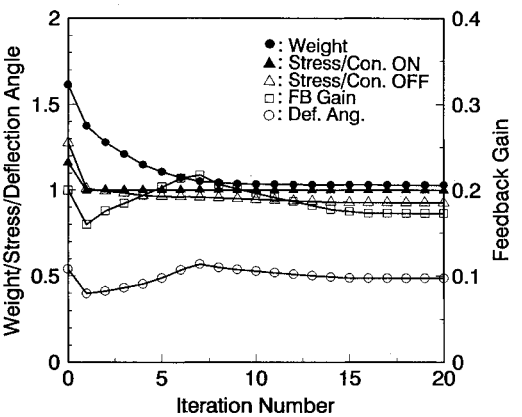

Fig. 11 Design cycle histories of objective functions (in Fig. 9) obtained from different starting points (uniform spar).

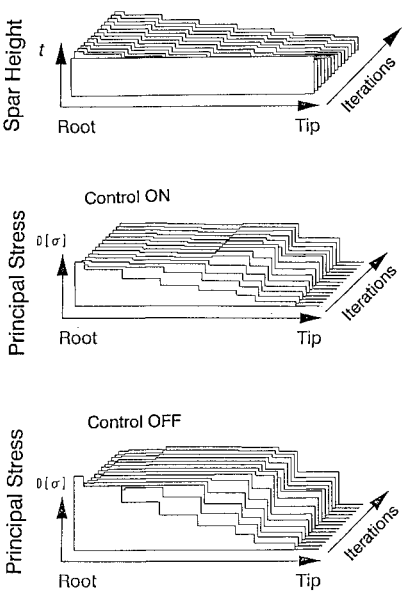

Fig. 12 Design cycle history of spar height and principal stress with control system on/off (control/structure optimization with stability margin).

shows the iteration histories of the element spar height and the principal stress with the control system on and off. Note that as the spar height changes from a uniform spar, the principal stresses with the control system on and off are kept within their allowable limits.

Conclusion

A simultaneous structure/control design optimization of a wing structure with a GLA system was presented. The structural weight was minimized with the following structure and control design requirements: 1) system stability requirements incorporating stability margins; 2) gust-induced stress constraints with the control system on or off; and 3) restriction of the control surface deflection angle. The gust-induced stress and the control surface deflection angle were statistically evaluated by the standard deviation of a parameter in a time-domain formulation. To assure system stability margins, system stability was guaranteed by allowing the feedback gain to increase the design variable by up to 3.16 times. Numerical examples demonstrate the successful application of a GP formulation for structure/control simultaneous design by comparing the results to a conventional design (i.e., only structure design parameters are initially optimized without considering the control system), and then the controller feedback gain is adjusted. Further investigations are necessary to treat more complex multiple input and multiple output (MIMO) control systems and also to consider practical wing design requirements such as flutter and structure failure characteristics in addition to the gust-induced stress. Although analytical derivatives of aerodynamic loads can be obtained with the presented simple aerodynamic model, future studies are needed to address full nonsteady or transonic flows.

References

[1]Ashley, H., "Flutter Suppression Within Reach," *Aerospace America*, Vol. 26, No. 8, 1988, pp. 14–16.

[2]Weissharr, T. A., "Coupling Structure and Control Design," *Aerospace America*, Vol. 26, No. 8, 1988, pp. 18–20.

[3]ACT Study Group, "Gust Load Alleviation of a Cantilevered Rectangular Elastic Wing. Wind Tunnel Experiment and Analysis," (in Japanese) National Aerospace Lab., TR-846, Tokyo, 1984.

[4]NASA/DOD Control-Structures Interaction Technology 1989, Compiled by J. R. Newsom, NASA CP-3041, Aug. 1989.

[5]Haftka, R. T., "Structural Optimization with Aeroelastic Constraints: A Survey of US Applications," *International Journal of Vehicle Design*, Vol. 7, Nos. 3 and 4, 1986, pp. 381–392.

[6]Rao, S. S., "Automated Optimum Design of Wing Structures: A Probabilistic Approach," *Computers and Structures*, Vol. 24, No. 5, 1986, pp. 799–808.

[7]Hajela, P., and Bach, C. T., "Optimum Structural Sizing for Gust-Induced Response," *Journal of Aircraft*, Vol. 26, No. 4, 1989, pp. 395–397.

[8]Mukhopadhyay, V., Newsom, J. R., and Abel, I., "A Method for Obtaining Reduced Order Control Laws for High Order Systems Using Optimization Technique," NASA TP-1876, Aug. 1981.

[9]Liebst, B. S. Garrard, W. L., and Farm, J. A., "Design of Multivariable Flutter Suppression/Gust Load Alleviation System," *Journal of Guidance and Control*, Vol. 11, No. 3, 1988, pp. 220–229.

[10]Zeiler, T. A., and Weisshaar, T. A., "Integrated Aeroservoelastic Tailoring of Lifting Surface," *Journal of Aircraft*, Vol. 25, No. 1, 1988, pp. 76–83.

[11]Suzuki, S., and Matsuda, S., "Structure/Control Design Synthesis of Active Flutter Suppression System by Goal Programming," *Journal of Guidance and Control*, Vol. 14, No. 6, 1991, pp. 1260–1266.

[12]Karpel, M., "Sensitivity Derivatives of Flutter Characteristics and Stability Margins for Aeroservoelastic Design," *Journal of Aircraft*, Vol. 27, No. 4, 1990, pp. 368–375.

[13]Ignizo, J. P., *Goal Programming and Extensions*, Heath, Boston, MA, 1976.

[14]Kwakernaak, K., and Sivan, R., *Linear Optimal Control Systems*, Wiley, New York, 1972, pp. 97–113.

[15]Zienkiewicz, O. C., *The Finite Element Method in Engineering Science*, McGraw-Hill, Berkshire, England, UK, 1971, pp. 16–32.

[16]Kreisselmeier, G., and Steinhauser, R., "Systematic Control Design by Optimizing a Vector Performance Index," *Proceedings of IFAC Symposium on Computer Aided Design of Control Systems*, Zurick, Pergamon, Oxford, England, UK, 1979, pp. 113–117.

[17]Haftka, R. T., Gürdal, Z., and Kamat, M. P., *Elements of Structural Optimization*, 2nd ed., Kluwer Academic Publishers, Dordrecht, 1990, pp. 189–193.

[18]Haug, E. J., Choi, K. K., and Komkov, V., *Design Sensitivity Analysis of Structural Systems*, Academic Press, London, 1985, pp. 49–70.

[19]Nelson, R. B., "Simplified Calculation of Eigenvector Derivatives," *AIAA Journal*, Vol. 14, No. 9, 1976, pp. 1201–1205.